Journal of Engineering Mathematics **38:** 33–50, 2000.

The ac-dc difference of single-junction thermal converters

V. BUBANJA*
New Zealand Institute for Industrial Research and Development, PO Box 31-310, Lower Hutt, New Zealand; e-mail: (v.bubanja@irl.cri.nz)

Received 19 June 1998; accepted in revised form 15 June 1999

Abstract. A nonlinear parabolic partial differential equation of heat conduction subject to the Robin boundary conditions is considered. The equation describes energy conservation in the heater wire of a single-junction thermal converter for both ac and dc currents. In the audio-frequency range the temperature distribution along the heater is calculated and the ac-dc difference deduced by means of the Picard iterative technique. The previously neglected effects of radiation and the thermal properties of the heater wire are included. An expression for the ac-dc difference is also derived in the low-frequency regime. The thermal conductance of the thermocouple, which has previously been neglected, is taken into account. The calculated increase in the ac-dc difference is consistent with recent measurements. The solution in this limit is found by both an eigenfunction-expansion method and the Laplace-transform method. Comparison of the solutions obtained by the two methods gives some useful formulae for the summation of numerical series.

Key words: alternating current standard, single junction thermal converters, heat conduction

1. Introduction

In most national standards laboratories the realisation of the dc electrical quantities is based on the Josephson and the quantum Hall effects. The fundamental realisation of ac quantities is performed by means of thermal converters, where the effect of the ac rms value and an equivalent dc value can be compared in turn. Such a definition is completely dependent on the accurate modelling of the intrinsic performance of the thermal device to correct for any difference in its response between ac and dc.

In this paper we discuss the operation of the single-junction thermal converter (SJTC), schematically shown in Figure 1. It consists of a straight heater wire, about 5 mm long and 10 μm wide, usually made of Evanohm or Nichrome alloys. The lead-in wires are about 25 times larger in diameter, so that the Joule heat generated by the current occurs almost entirely in the heater region. The mid-point temperature of the heater is sensed by a thermocouple attached to the heater, often by means of a small ceramic bead. The amplitude of an unknown ac current can then be adjusted, so that the output voltage of the thermocouple is the same as that obtained for a known dc reference current. This implies that the rms of the input ac current is approximately equal to the input dc current. However, owing to the presence of non-Joule heating and the temperature dependence of the heater properties, there will be a small difference between the dc and ac signals required to give the same output. This ac-dc difference of the thermal converter is defined as

* Currently at: Electrotechnical Laboratory, Electron Devices Division, 1-1-4 Umezono, Tsukuba, Ibaraki, 305-8568 Japan.

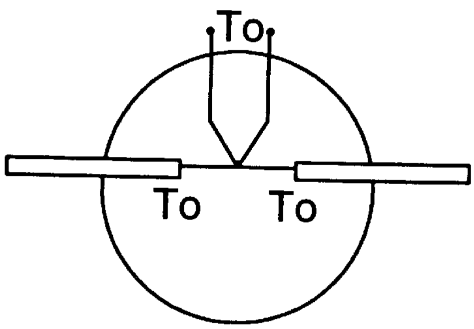

Figure 1. Model of a SJTC.

$$\delta = \frac{I_{ac} - I_{dc}}{I_{dc}}, \qquad (1)$$

where I_{ac} and I_{dc}[1] are the rms ac and dc input currents that produce the same output of the thermocouple.

The thermocouple operation is based on the Seebeck effect, giving an output voltage proportional to the increase of the midpoint temperature of the heater. Joule heat produced by the current is conducted through the support leads and irradiated into the surroundings. Depending on the direction of the current with respect to the temperature gradient, Thomson heat is emitted or absorbed from the surroundings. Part of the heat is also conducted through the bead and down the thermocouple.

The most accurate measurements of ac currents and voltages are performed at audio frequencies (20 Hz to 20 kHz) and in this range the international comparisons of base ac standards are carried out. However, there is an increasing need from industry for accurate ac measurements at low frequencies (below about 20 Hz). We consider both ranges in this paper.

In the audio range the temperature along the heater is stationary owing to the thermal inertia of the wire. The main cause of the ac-dc difference in this range is due to the Thomson effect which is present in the dc but not in the ac case. In [3] this frequency range has been considered, but the important fact that heat is also conducted along the thermocouple has been neglected. In [1] the thermocouple has been taken into account, but the Thomson coefficient, which is proportional to the absolute temperature, has been assumed constant. Both treatments neglect the radiation and the temperature dependence of the electrical and thermal properties of the heater.

In the low-frequency range the temperature starts to follow the oscillations of the power released in the wire. The average value over an integral number of cycles does not coincide with the temperature value in the dc case due to the nonlinearities in the heat flow equation. In the previous considerations of this aspect of the problem [3] the heat conducted along the thermocouple has been neglected. Here we derive a complete solution in both the audio and the low frequency ranges.[2] The expressions derived in terms of all the parameters involved

[1] In the practice if the thermocouple is not attached to the middle of the heater it's response would be different for the two directions of the dc current, the so-called reversal error [1], [2]. However, for the most accurate measurements one can select only those SJTCs with negligible reversal error, and therefore in our model we will assume that the ceramic bead is attached to the center of the heater wire.

[2] The Peltier effect ([1], [2], [4]) due to the different materials used in the heater and support leads is not discussed in this paper. This can be considered in addition to the present model.

will be useful for the detailed analysis of SJTCs used to provide standards of ac quantities, and in the design in high accuracy devices.

2. Mathematical description of the problem

The temperature distribution in the heater wire is governed by the following heat-flow equation [5]

$$\frac{\partial}{\partial x}\left(ak\frac{\partial T}{\partial x}\right) - \alpha_T I\frac{\partial T}{\partial x} + \frac{I^2\rho}{a} - p\varepsilon\sigma(T^4 - T_0^4) = ams\frac{\partial T}{\partial t}. \tag{2}$$

The four terms on the left hand side are due to conduction, Thomson heating or cooling (with $\alpha_T = \beta_T T$ where β_T is a constant for each material), Joule heating, and radiation, respectively (a table of symbols is at the end of the article). The right-hand term is the rate of heat gained by an infinitesimal element of the heater. In order to reduce convection, the SJTC is usually placed in an evacuated glass envelope. The temperature at the end points of the heater wire is fixed at the room temperature T_0. Due to the thermal conductance of the thermocouple bead, there is a heat sink at the mid-point of the heater[3]. This means that (2) is to be solved on the intervals $-l \leqslant x \leqslant 0$ and $0 \leqslant x \leqslant l$ subject to the boundary conditions:

$$\begin{aligned} &T(\pm l, t) = T_0, \qquad T(0-, t) = T(0+, t), \\ &\left.\frac{\partial T}{\partial x}\right|_{x\to 0-} - \left.\frac{\partial T}{\partial x}\right|_{x\to 0+} = -\frac{K}{ak}(T(0,t) - T_0), \end{aligned} \tag{3}$$

and the initial condition

$$T(x, 0) = T_0. \tag{4}$$

The temperature dependence of the heater properties (resistivity, thermal conductivity, and specific heat) are as follows:

$$\rho = \rho_0(1 + \alpha(T - T_0)), \quad k = k_0(1 + \beta(T - T_0)), \quad s = s_0(1 + \zeta(T - T_0)). \tag{5}$$

For the currents of interest (typically a few milliamps) the maximum temperature increase along the heater is of the order of magnitude of 100 K. In this case the Thomson and radiation terms in (2) are much less than the Joule heating, and $\alpha(T - T_0), \beta(T - T_0), \zeta(T - T_0) \ll 1$. We therefore treat all these terms perturbatively. In order to find δ, we solve the above equation for the temperature distribution and compare the mid-point temperature value in the dc and ac cases. We distinguish two frequency ranges of the ac input: the audio range where the temperature does not oscillate (from about 20 Hz to 20 kHz and low frequencies where the temperature follows the oscillations of the input signal (typically below 20 Hz).

3. Audio-frequency range

We first consider the above Equation (2) for the dc case. Since we are interested in the stationary solution ($t \gg msl^2/k$), we put the right-hand side equal to zero. If we take only the

[3] In principle, apart from conduction, there is also radiation loss along the thermocouple. However, without current in the thermocouple the resulting temperature distribution is linear. Therefore this component of the heat loss effectively only increases the thermal conductance of the thermocouple.

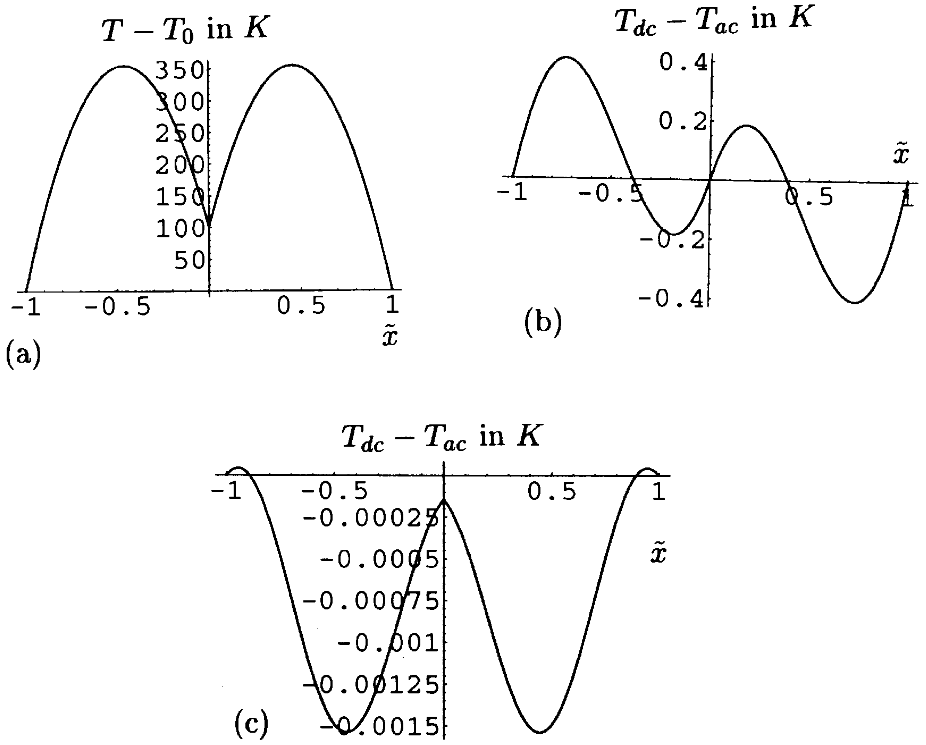

Figure 2. The zeroth (a), first (b) and second (c) order of perturbation. $T_0 = 291\,\text{K}$, $\beta_T = 0{\cdot}25 \times 10^{-8}\,\text{V/K}^2$, $\rho_0 = 1{\cdot}34 \times 10^{-6}\,\Omega\text{m}$, $k_0 = 14\,\text{W/(mK)}$, $N = 12$, $l = 2{\cdot}5 \times 10^{-3}\,\text{m}$, $as = 7{\cdot}85 \times 10^{-11}\,\text{m}^2$.

Thomson term as a nonlinearity the equation can be solved exactly (Appendix A). However, if radiation and the temperature dependence of the heater properties are included we have to resort to approximation methods. Here we use the Picard iterative procedure [6], rewriting (2) as

$$\frac{\mathrm{d}^2T}{\mathrm{d}\tilde{x}^2} = -B - WT\frac{\mathrm{d}T}{\mathrm{d}\tilde{x}} - \eta B_1 T - RT_4 - \beta\left(\frac{\mathrm{d}T}{\mathrm{d}\tilde{x}}\right)^2, \tag{6}$$

where

$$B = B_1(1-\eta T_0) - RT_0^4, \qquad B_1 = \frac{I_{\mathrm{dc}}^2\rho_0 l^2}{a^2k_0}, \qquad R = \frac{p\varepsilon\sigma l^2}{ak_0},$$

$$W = -\frac{\beta_T I_{\mathrm{dc}} l}{ak_0}, \qquad \eta = \alpha - \beta, \qquad \tilde{x} = \frac{x}{l}. \tag{7}$$

For the zeroth order of iteration we take $W = \eta = R = \beta = 0$ in (6). The first order is then obtained by solving (6) with $T(\tilde{x})$ on the right-hand side approximated by the zeroth order solution. The resulting linear differential equation is then straightforward to solve.

The temperature distribution for an ac current is also obtained iteratively from (6) with $W = 0$ (in this case the Thomson term is proportional to the sinusoidal current; its contribution to the solution will be of amplitude inversely proportional to the angular frequency of the current so for $\omega \gg k/msl^2$ the contribution of this forcing term can be neglected). An example of the iterative solution is shown in Figure 2. Both the dc and ac currents produce the same zeroth-order temperature distribution (graph (a) on the figure). The difference between the dc and ac distributions in the first-order iteration (graph (b)) is symmetric about the origin and therefore we proceed to the second order of perturbation (graph (c)) where there is a difference between dc and ac temperatures at the mid-point. This gives rise to a nonzero value of δ.

Since the results are of the form $T_{ac} - T_0 = a_2 I_{ac}^2 + a_4 T_{ac}^4 + \cdots$ and $T_{dc} - T_0 = a_2 I_{dc}^2 + b_4 T_{dc}^4 + \cdots$ and $a_4, b_4 \ll a_2$ we can rewrite (1) to read:

$$\delta = -\frac{T_{ac} - T_{dc}}{2(T_{dc} - T_0)}, \tag{8}$$

where T_{ac} and T_{dc} are the mid-point temperatures in the ac and dc cases for $I_{ac} = I_{dc}$. Using the second-order results for the mid-point temperature, we obtain[4]

$$\begin{aligned}\delta \;=\; & \frac{\beta_T^2 T_0^2 R_{h0}^2}{32(\rho_0 k_0)^2 (4RT_0^3 + N(3 + RT_0^3))} I^2 - \frac{\beta_T^2 T_0^2 R_{h0}^2 (15 + 4N)}{3840N(\rho_0 k_0)^3 (4RT_0^3 + N(3 + RT_0^3))} I^4 \\ & - \frac{\beta_T^2 R_{h0}^6 (4 + N)^2}{122880N^2(\rho_0 k_0)^4 (4RT_0^3 + N(3 + RT_0^3))} I^6, \end{aligned} \tag{9}$$

where R_{h0} is the heater resistance at T_0 and $N = 1 + K/(2ak/l)$. We may reduce the above Equation (9) to the result of Hermach [3] for $N = 1$, $R = 0$, and to the result of Widdis [1] assuming the Thomson coefficient to be constant and taking $R = 0$. Inglis developed a method [7] for measuring the coefficients in the expansion $\delta(I) = c_2 I^2 + c_4 I^4 + c_6 I^6 + \cdots$. The results were in general agreement with (9), but fluctuations were also present due to the nonhomogeneities in the heater material. The results for some typical values of heater wires are shown in Figures 3 and 4. In the existing literature radiation has only been taken into account in [8] where a simplified version of Equation (2) has been solved by a finite difference scheme. The author concluded that radiation losses might be more important to ac-dc difference than was previously understood. We can conclude from (9) that the relative error caused by not taking the radiation into account is given by

$$\frac{\delta_{R=0} - \delta}{\delta_{R=0}} \sim RT_0^3 \frac{N + 4}{3N}.$$

It is hoped that this, as well as the formula (9), will be useful for the designers of SJTC.

Comment: In solving Equation (6) we have assumed that nonlinear terms act as perturbations, and *a posteriori* verified that (the first- and second-order effects are decreasing by several orders of magnitude). Alternatively, we can get the same result by rewriting (6) (to simplify the expressions below we take the case $\beta = \eta = 0$) as

$$\frac{d^2}{d\tilde{x}^2}\left(\frac{T}{T_0}\right) = -\mu^2 + \gamma\mu\left(\frac{T}{T_0}\right)\frac{d}{d\tilde{x}}\left(\frac{T}{T_0}\right) + \psi\left(\left(\frac{T}{T_0}\right)^4 - 1\right), \tag{10}$$

where

$$\mu = \frac{R_{ho} I_{dc}}{2\sqrt{\rho_0 k_0 T_0}}, \qquad \gamma = \frac{\beta_T T_0^{3/2}}{\sqrt{\rho_0 K_0}}, \quad \text{and} \quad \psi = \frac{p \in \sigma l^2 T_0^3}{a k_0}.$$

[4] Since the number of terms in the iterative process gets very large we use Mathematica software.

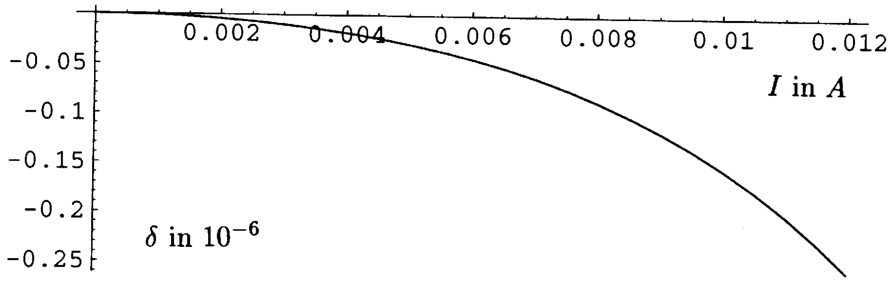

Figure 3. δ as a function of the heater current for an Evanohm heater for: $T_0 = 291\,\mathrm{K}$, $\beta_T = 0{\cdot}25 \times 10^{-8}\,\mathrm{V/K}^2$, $\rho_0 = 1{\cdot}34 \times 10^{-6}\,\Omega\mathrm{m}$, $k_0 = 14\,\mathrm{W/(mk)}$, $a = 3{\cdot}14 \times 10^{-10}\,\mathrm{m}^2$, $\varepsilon = 0{\cdot}3$, $l = 2{\cdot}5 \times 10^{-3}\,\mathrm{m}$; $N = 7$.

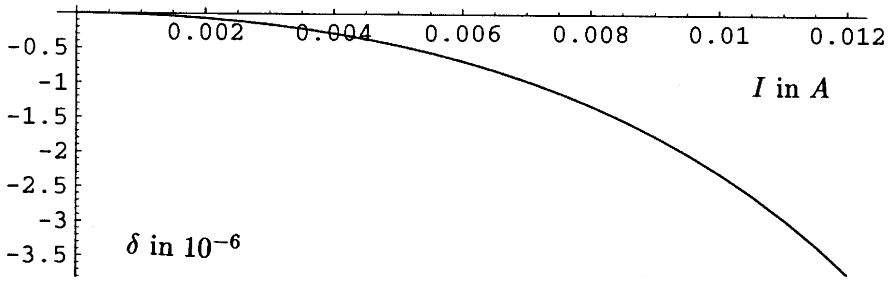

Figure 4. δ as a function of the heater current for an Nichrome heater for: $T_0 = 291\,\mathrm{K}$, $\beta_T = 10^{-8}\,\mathrm{V/K}^2$, $\rho_0 = 1{\cdot}08 \times 10^{-6}\,\Omega\mathrm{m}$, $k_0 = 14\,\mathrm{W/(mk)}$, $a = 3{\cdot}14 \times 10^{-10}\,\mathrm{m}^2$, $\varepsilon = 0{\cdot}3$, $l = 2{\cdot}5 \times 10^{-3}\,\mathrm{m}$; $N = 7$.

We search for the solution in the form

$$\frac{T}{T_0} = \sum_{i=0}^{\infty} c_i(\tilde{x})\mu^1. \tag{11}$$

By substituting (11) in (10) we obtain a set of equations for $c_i(\tilde{(}x)$

$$\sum_{i=0}^{\infty}\left(\frac{\mathrm{d}^2c_i}{\mathrm{d}\tilde{x}^2} + \delta_{i,2} - ga\sum_{j=0}^{i-1} c_{i-j-1}\frac{\mathrm{d}c_j}{\mathrm{d}\tilde{x}} - \psi\sum_{j=0}^{i}\sum_{k=0}^{i-j}\sum_{l=0}^{j} c_{i-k-j}c_kc_{j-l}c_l + \psi\delta_{i,0}\right)\mu^i = 0, \tag{12}$$

where $\delta_{i,j}$ is the Kronecker symbol and γ and ψ are small parameters. By substituting the solution of (12) in (11) and using (8) we obtain (9).

4. Low-frequency range

Owing to the thermal inertia of the heater wire, the temperature does not follow the oscillations of the source in the audio-frequency range. However at low frequencies the temperature does oscillate. We are interested in the average value of these oscillations, which, because of the nonlinearities of the heat equation, does not coincide with the temperature in the dc case. In the audio range we obtained a difference between ac and dc cases in the second order of iteration. At low frequencies there is already first-order difference. The Thomson term does not cause a change in the mid-point temperature for dc at this order and the average over the period of ac oscillations of this term is zero. Therefore we omit the Thomson term below. Since we are modeling a stable physical situation we have a well-posed problem. As above we will treat the same small terms perturbatively. In the zeroth order of approximation, we rewrite (2) in the form

$$\frac{\partial^2 u}{\partial x^2} - \frac{1}{\tilde{k}}\frac{\partial u}{\partial t} = -\frac{A_0}{\tilde{k}}, \tag{13}$$

where

$$u = T - T_0, \qquad \tilde{k} = \frac{k_0}{ms_0}, \qquad A_0 = \frac{I^2\rho_0}{a^2 ms_0}. \tag{14}$$

For the dc case, $I = I_{\mathrm{dc}}$ in the above equation. Since (13) is symmetric with respect to the variable x, we solve the equation for $-l \leqslant x \leqslant 0$ only. The boundary conditions are

$$u(-l,t) = 0, \qquad \left.\frac{\partial u}{\partial x}\right|_{x\to 0-} = -hu(0,t), \tag{15}$$

where $h = K/(2ak)$. A separation of variables construction yields

$$\begin{aligned} u(x,t) \;=\; & -\frac{A_0 x^2}{2\tilde{k}} - \frac{A_0 l^2}{2\tilde{k}}\frac{hx}{1+hl} + \frac{A_0 l^2}{2\tilde{k}}\frac{1}{1+hl} \\ & + \frac{4A_0 l^2}{\tilde{k}}\sum_{n=1}^{\infty}\exp(-\tilde{k}\alpha_n^2 t)\frac{(1-\cos(\alpha_n l))\sin(\alpha_n(x+l))}{(\alpha_n l)^2(\sin(2\alpha_n l) - 2\alpha_n l)}, \end{aligned} \tag{16}$$

where the eigenvalues α_n satisfy the condition

$$\tan(\alpha_n l) = -\frac{\alpha_n l}{hl}. \tag{17}$$

The exponentially decaying terms in (16) are simply transients for the pupose of the present discussion, but they are of interest in the study of time constants of thermoelectric effects [9]–[11].

For the ac case with $I^2 = T_{\mathrm{rms}}^2(1-\cos(2\omega t))$, we rewrite (2) to read

$$\frac{\partial^2 u}{\partial x^2} - \frac{1}{\tilde{k}}\frac{\partial u}{\partial t} = -\frac{A_0}{\tilde{k}} + \frac{A_0}{\tilde{k}}\cos(2\omega t), \tag{18}$$

with variables defined as in (14) with $I = I_{\mathrm{rms}}$ in the expression for A_0. We separate the time independent term by writing

$$u(x,t) = v(x,t) + w(x), \tag{19}$$

where

$$w(x) = -\frac{A_0 x^2}{2\tilde{k}} - \frac{A_0 l^2}{2\tilde{k}} + \frac{hx}{1+hl} + \frac{A_0 l^2}{2\tilde{k}}\frac{1}{1+hl}. \tag{20}$$

The equation for v is

$$\frac{\partial^2 v}{\partial x^2} - \frac{1}{\tilde{k}}\frac{\partial v}{\partial t} = \frac{A_0}{\tilde{k}}\cos(2\omega t), \tag{21}$$

After performing the Laplace transform we obtain from (21)

$$\frac{\partial^2 \tilde{v}}{\partial x^2} - \frac{1}{\tilde{k}} s\tilde{v} = \frac{A_0}{\tilde{k}}\frac{s}{s^2+(2\omega)^2} - \frac{A_0}{2\tilde{k}^2}\left(x^2 + \frac{hxl^2}{1+hl} - \frac{l^2}{1+hl}\right), \tag{22}$$

where:

$$\tilde{v}(x,s) = \int_0^\infty \mathrm{d}t\, \mathrm{e}^{-st} v(x,t). \tag{23}$$

The solution of (22) subject to the boundary conditions

$$\tilde{v}(-l,s) = 0, \qquad \left.\frac{\mathrm{d}\tilde{v}}{\mathrm{d}x}\right|_{x\to 0-} = -h\tilde{v}(0,s), \tag{24}$$

is

$$\begin{aligned}\tilde{v}(x,s) &= A_0\left(\frac{1}{s^2} - \frac{1}{s^2+(2\omega)^2}\right)\\ &\times\left(1 - \frac{\sqrt{\frac{s}{\tilde{k}}}\cosh\left(\sqrt{\frac{s}{\tilde{k}}}x\right) - h\sinh\left(\sqrt{\frac{s}{\tilde{k}}}x\right) + h\sinh\left(\sqrt{\frac{s}{\tilde{k}}}(x+l)\right)}{\sqrt{\frac{s}{\tilde{k}}}\cosh\left(\sqrt{\frac{s}{\tilde{k}l}}l\right) + h\sinh\left(\sqrt{\frac{s}{\tilde{k}}}l\right)}\right)\\ &+\frac{A_0}{2s\tilde{k}}\left(x^2 + \frac{hxl^2}{1+hl} - \frac{l^2}{1+hl}\right).\end{aligned} \tag{25}$$

By performing the inverse Laplace transform, we have

$$\begin{aligned}v(x,t) &= -\frac{A_0}{2\omega}\sin(2\omega t) + A_0\frac{1}{2\pi i}P.V.\int_{\gamma-i\infty}^{\gamma+i\infty}\mathrm{d}s\,\mathrm{e}^{st}\frac{1}{s^2+(2\omega)^2}\\ &\times\frac{\sqrt{\frac{s}{\tilde{k}}}\cosh\left(\sqrt{\frac{s}{\tilde{k}}}x\right) - h\sinh\left(\sqrt{\frac{s}{\tilde{k}}}x\right) + h\sinh\left(\sqrt{\frac{s}{\tilde{k}}}(x+l)\right)}{\sqrt{\frac{s}{\tilde{k}}}\cosh\left(\sqrt{\frac{s}{\tilde{k}}}l\right) + h\sinh\left(\sqrt{\frac{s}{\tilde{k}}}l\right)}\\ &+A_0 t - A_0\frac{1}{2\pi i}P.V.\int_{\gamma-i\infty}^{\gamma+i\infty}\mathrm{d}s\,\mathrm{e}^{st}\frac{1}{s^2}\\ &\times\frac{\sqrt{\frac{s}{\tilde{k}}}\cosh\left(\sqrt{\frac{s}{\tilde{k}}}x\right) - h\sinh\left(\sqrt{\frac{s}{\tilde{k}}}x\right) + h\sinh\left(\sqrt{\frac{s}{\tilde{k}}}(x+l)\right)}{\sqrt{\frac{s}{\tilde{k}}}\cosh\left(\sqrt{\frac{s}{\tilde{k}}}l\right) + h\sinh\left(\sqrt{\frac{s}{\tilde{k}}}l\right)}\\ &+\frac{A_0}{2\tilde{k}}\left(x^2 + \frac{hxl^2}{1+hl} - \frac{l^2}{1+hl}\right).\end{aligned} \tag{26}$$

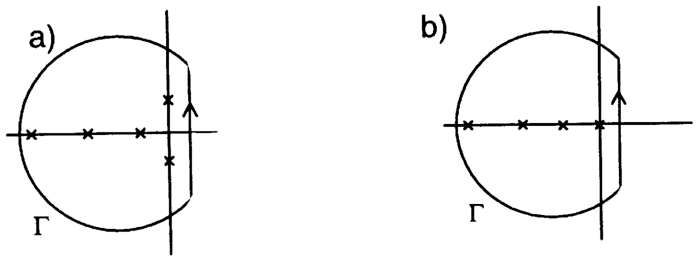

Figure 5. Poles and contours of integration for integrals in (39).

In order to establish whether the integrands above are meromorphic functions in the complex s-plane, we investigate the zeros of the term in the denominator

$$\sqrt{\frac{s}{\tilde{k}}}\cosh\left(\sqrt{\frac{s}{\tilde{k}}}l\right) + h\sinh\left(\sqrt{\frac{s}{\tilde{k}}}l\right) = 0. \tag{27}$$

We can divide this equation by $\cosh\left(\sqrt{\frac{s}{\tilde{k}}}\right) \neq 0$ (if $\cosh\left(\sqrt{\frac{s}{\tilde{k}}}\right) = 0$ one can verify that $\sinh\left(\sqrt{\frac{s}{\tilde{k}}}\right) \neq 0$, so then (27) is not satisfied) to obtain

$$\tanh\left(\sqrt{\frac{s}{\tilde{k}}}l\right) = -\frac{\sqrt{\frac{s}{\tilde{k}}}l}{hl}. \tag{28}$$

By denoting $\sqrt{\frac{s}{\tilde{k}}}l = a + \mathrm{i}b$, and equating the real and imaginary parts of both sides, we have

$$\frac{\sinh(2a)}{\cosh(2a)+\cos(2b)} = -\frac{a}{hl}, \tag{29}$$

$$\frac{\sin(2b)}{\cosh(2a)+\cos(2b)} = -\frac{b}{hl}. \tag{30}$$

For $a \neq 0$ in (29) $\cosh(2a) > 1$ so that $\cosh(2a) + \cos(2b) > 0$. If $a > 0$ then the left-hand side of (29) is positive, but the right-hand side is negative, and vice versa if $a < 0$. Therefore, the equation is satisfied only for $a = 0$. Then (30) reduces to:

$$\tan(b) = -\frac{b}{hl}. \tag{31}$$

Since $b = \mathfrak{Im}\left(\sqrt{\frac{s}{\tilde{k}}}l\right)$, $a = 0$, and $\sqrt{\frac{1}{\tilde{k}}}l > 0$, we have that the solutions of (31) are found for $s < 0$, and they are positive: $b > 0$. Solution $b = 0$ of (31) is not included since:

$$\lim_{s\to 0}\frac{\sqrt{\frac{s}{\tilde{k}}}\cosh\left(\sqrt{\frac{s}{\tilde{k}}}x\right) - h\sinh\left(\sqrt{\frac{s}{\tilde{k}}}x\right) + h\sinh\left(\sqrt{\frac{s}{\tilde{k}}}(x+l)\right)}{\sqrt{\frac{s}{\tilde{k}}}\cosh\left(\sqrt{\frac{s}{\tilde{k}}}l\right) + h\sinh\left(\sqrt{\frac{s}{\tilde{k}}}l\right)} = 1. \tag{32}$$

The poles of the first integrand are shown in Figure 5(a), and of second integrand in Figure 5(b). In both cases there are infinitely many poles along the negative real s-axis, but since the poles are distributed as

$$s_n \sim -\frac{\tilde{k}\pi^2}{l^2}(n-1/2)^2 \quad \text{for } n \to \infty,$$

we can always find a curve Γ between them. It is easy to see that integral along Γ vanishes, and so we can use the residue theorem to evaluate the Bromwich integrals in (26).

After some algebra, we obtain

$$\begin{aligned}
v(x,t) = & -\frac{A_0}{2\omega}\sin(2\omega t) \\
& +\frac{A_0}{2\omega}((\gamma(\sinh(\gamma l)\sin(\gamma l)-\cosh(\gamma l)\cos(\gamma l))-h\sinh(\gamma l)\cos(\gamma l))^2 \\
& +(\gamma(\cosh(\gamma l)\cos(\gamma l)+\sinh(\gamma l)\sin(\gamma l))+h\cosh(\gamma l)\sin(\gamma l))^2)^{-1} \\
& \times((\tfrac{1}{2}((h^2+2\gamma^2)\cos(\gamma(x+l))\cosh(\gamma(x-l)) \\
& \qquad -h^2\cos(\gamma(x-l))\cosh(\gamma(x+l))+2\gamma^2\cos(\gamma(x-l))\cosh(\gamma(x+l)) \\
& \qquad +h^2\cos(\gamma x)\cosh(\gamma(x+2l))))\sin(2\omega t)-2h\gamma\cosh(\gamma(x+l))\sin(\gamma(x-l)) \\
& +h\gamma\cosh(\gamma(x+2l))\sin(\gamma x)-h\cosh(\gamma x)(h\cos(\gamma(x+2l)) \\
& -\gamma\sin(\gamma(x+2l))-2h\gamma\cos(\gamma(x+l))\sinh(\gamma(x-l)) \\
& +h\gamma\cos(\gamma(x+2l))\sinh(\gamma x)+h\gamma\cos(\gamma x)\sinh(\gamma(x+2l))))\sin(2\omega t) \\
& +(\tfrac{1}{2}(h\gamma\cosh(\gamma(x+2l))\sin(\gamma x)-2h\gamma\cosh(\gamma(x-l))\sin(\gamma(x+l)) \\
& +h\gamma\cosh(\gamma x)\sin(\gamma(x+2l))+h^2\sin(\gamma(x+l))\sinh(\gamma(x-l)) \\
& +2\gamma^2\sin(\gamma(x+l))\sinh(\gamma(x-l))-h\gamma\cos(\gamma(x+2l)\sinh(\gamma x) \\
& -h^2\sin(\gamma(x+2l))\sinh(\gamma x)+2h\gamma\cos(\gamma(x-l))\sinh(\gamma(x+l)) \\
& -h^2\sin(\gamma(x-l))\sinh(\gamma(x+l))+2\gamma^2\sin(\gamma(x+l))\sinh(\gamma(x-l)) \\
& -h\gamma\cos(\gamma(x+2l))\sinh(\gamma x)-h^2\sin(\gamma(x+2l))\sinh(\gamma x) \\
& +2h\gamma\cos(\gamma(x-l))\sinh(\gamma(x+l))-h^2\sin(\gamma(x-l))\sinh(\gamma(x+l)) \\
& +2\gamma^2\sin(\gamma(x-l))\sinh(\gamma(x+l))-h\gamma\cos(\gamma x)\sinh(\gamma(x+2l)) \\
& +h^2\sin(\gamma x)\sinh(\gamma(x+2l))))\cos(2\omega t)
\end{aligned}$$

$$+\frac{4A_0}{\tilde{k}}\sum_{n=1}^{\infty}\frac{1-\cos(\alpha_n l)}{\sin(2\alpha_n l)-2\alpha_n l}\frac{(2\omega)^2}{\alpha_n^2(\alpha_n^4\tilde{k}^2+(2\omega)^2}\mathrm{e}^{-\alpha_n^2\tilde{k}^2 t}\sin(\alpha_n(x+l)), \tag{33}$$

where $\gamma = \sqrt{\omega/\tilde{k}}$ and $\alpha_n l$ denote the solutions of (31). From here, we have for the temperature increase in the stationary state ($t \to \infty$)

$$u(x,t) = w(x) + f(x)\cos(2\omega t) + g(x)\sin(2\omega t), \tag{34}$$

where $w(x)$ is also the steady state solution in the dc case, and $f(x)$ and $g(x)$ are the coefficients of $\cos(2\omega t)$ and $\sin(2\omega t)$ in (33). The temperature oscillates with twice the frequency of the input signal, but, if we average (34) over an integral number of cycles, we have that the midpoint temperature increase coincides with that for the dc case: $\overline{u(0,t)} = w(0)$. Therefore, we proceed to the first order approximation, that is, we rewrite (2) for the dc case as:

$$\frac{\partial^2 u}{\partial x^2} - \left(\frac{1}{\tilde{k}} + \frac{\zeta-\beta}{\tilde{k}}u\right)\frac{\partial u}{\partial t}$$
$$= -\frac{A_0}{\tilde{k}} - \beta\left(\frac{\partial u}{\partial x}\right)^2 - \eta\frac{A_0}{\tilde{k}}u - \frac{R}{l^2}(u^4 + 4u^3T_0 + 6u^2T_0^2 + 4uT_0^3). \tag{35}$$

Since we are looking for the stationary solution, we take the time derivative equal to zero and on the right-hand side assume that the temperature increase is equal to the zeroth-order solution $u = w(x)$. Similarly, for the ac case we can write:

$$\frac{\partial^2 u}{\partial x^2} - \frac{1}{\tilde{k}}\frac{\partial u}{\partial t} = -\frac{A_0}{\tilde{k}} + \frac{A_0}{\tilde{k}}\cos(2\omega t) - \beta\left(\frac{\partial u}{\partial x}\right)^2 - \eta\frac{A_0}{\tilde{k}}u(1-\cos(2\omega t))$$
$$-\frac{R}{l^2}(u^4 + 4u^3T_0 + 6u^2T_0^2 + 4uT_0^3) + \frac{\zeta-\beta}{\tilde{k}}u\frac{\partial u}{\partial t}. \tag{36}$$

After substituting (34) in the right-hand side of (36), averaging over an integral number of cycles, and comparing with Equation (35), we have for w_{diff} (the difference in the temperature increases between the ac and the dc case) the following equation:

$$\frac{\mathrm{d}^2 w_{\mathrm{diff}}}{\mathrm{d}x^2} = -\frac{\beta}{2}\left(\left(\frac{\mathrm{d}f}{\mathrm{d}x}\right)^2 + \left(\frac{\mathrm{d}g}{\mathrm{d}x}\right)^2\right)$$
$$+\frac{\eta}{2}\frac{A_0}{\tilde{k}}f(x) - \frac{R}{l^2}[3T_0^2(f^2(x)+g^2(x)) + 6T_0 w(x)(f^2(x)+g^2(x))$$
$$+3w^2(x)(f^2(x)+g^2(x)) + \tfrac{3}{8}(f^2(x)+g^2(x))^2], \tag{37}$$

with the boundary conditions:

$$w_{\mathrm{diff}}(-l) = 0,$$
$$\left.\frac{\mathrm{d}w_{\mathrm{diff}}}{\mathrm{d}x}\right|_{x\to 0-} = -h w_{\mathrm{diff}}(0). \tag{38}$$

Since T_0 is the room temperature in degrees Kelvin, it turns out after integration that we can neglect terms in the square brackets of (37) other than those proportional to T_0^2. We obtain the ac-dc difference from $\delta = -w_{\text{diff}}(0)/(2w(0))$. The result is

$$\delta = \frac{A_0 l^2}{\tilde{k}}(\eta\delta_\eta + \beta\delta_\beta + RT_0^2\delta_R),$$

$$\begin{aligned}
\delta_\eta &= \frac{A}{64(\gamma l)^4}(2\mathfrak{Re}(r_1(1+\gamma l - \mathrm{e}^{(1+\mathrm{i})\gamma l}) \\
&\quad - r_2(1-\gamma l - \mathrm{e}^{-(1-\mathrm{i})\gamma l})) - 2\gamma l \mathfrak{Im}(r_2 - r_2)),\\
\delta_\beta &= \frac{A^2}{256(\gamma l)^4}(|r_1|^2(1+2\gamma l - \mathrm{e}^{2\gamma l}) \\
&\quad + |r^2|^2(1-2\gamma l - \mathrm{e}^{-2\gamma l}) - 2\mathfrak{R}(r_1 r_2(1-\mathrm{e}^{2\mathrm{i}\gamma l})) + 4\gamma l \mathfrak{Im}(r_1 r_2)),\\
\delta_R &= \frac{1}{256(\gamma l)^6}(-96(\gamma l)^2 + 48A(\mathfrak{Im}(-r_1(1+2\gamma l - \mathrm{e}^{(1+\mathrm{i})\gamma l}) \\
&\quad - r_2(1-2\gamma l - \mathrm{e}^{-(1-\mathrm{i})\gamma l})) - \gamma l \mathfrak{Re}(r_1 + r_2)) \\
&\quad + 3A^2(|r_1|^2(1+2\gamma l - \mathrm{e}^{2\gamma l}) + |r_2|^2(1-2\gamma l - \mathrm{e}^{-2\gamma l}) \\
&\quad + 2\mathfrak{Re}(r_1 r_2(1-\mathrm{e}^{2\mathrm{i}\gamma l})) - 2\gamma l \mathfrak{Im}(r_1 r_2))),\\
A &= ((\gamma l \sinh(\gamma l)\sin(\gamma l) - \cosh(\gamma l)\cos(\gamma l)) - hl\sinh(\gamma l)\cos(\gamma l))^2 \\
&\quad + (\gamma l\cosh(\gamma l)\cos(\gamma l) + \sinh(\gamma l)\sin(\gamma l)) + hl\cosh(\gamma l)\sin(\gamma l))^2)^{-1},\\
r_1 &= hl(hl - \gamma l(1-\mathrm{i}))\,\mathrm{e}^{-2\gamma l} - hl(hl + \gamma l(1-\mathrm{i}))\,\mathrm{e}^{-2\gamma l} \\
&\quad + (2(\gamma l)^2 - (hl)^2 - 2\,\mathrm{i}h\gamma l^2)\,\mathrm{e}^{-(1-\mathrm{i})\gamma l} + (2(\gamma l)^2 + (hl)^2 + 2h\gamma l^2)\,\mathrm{e}^{(1-\mathrm{i})\gamma l},\\
r_2 &= -hl(hl + \gamma l(1+\mathrm{i}))\,\mathrm{e}^{2\gamma l} + hl(hl - \gamma l(1+\mathrm{i}))\,\mathrm{e}^{-2\gamma l} \\
&\quad + (-2(\gamma l)^2 - (hl)^2 + 2h\gamma l^2)\,\mathrm{e}^{-(1+\mathrm{i})\gamma l} + (-2(\gamma l)^2 + (hl)^2 + 2\,\mathrm{i}h\gamma l^2)\,\mathrm{e}^{(1+\mathrm{i})\gamma l}.
\end{aligned} \tag{39}$$

This expression is valid at all frequencies. In particular, we have that $\delta \to 0$ as $\omega \to \infty$, so we need to go to the next order of approximation, as indeed we have done, in the treatment of the audio frequency range. In the case $\gamma l > 5$, (39) can be slightly simplified by neglecting $\mathrm{e}^{-\gamma l}$ in all terms. If we take $h = 0$ (no thermocouple heat conductance), (39) reduces to the case considered in [3]. We present δ as a function of the source frequency in Figure 6 for some parameter values. This is in general agreement with the form of the measured data of reference [12], although exact agreement is difficult to obtain without detailed information on the construction of the device that was used (in particular the temperature characteristic

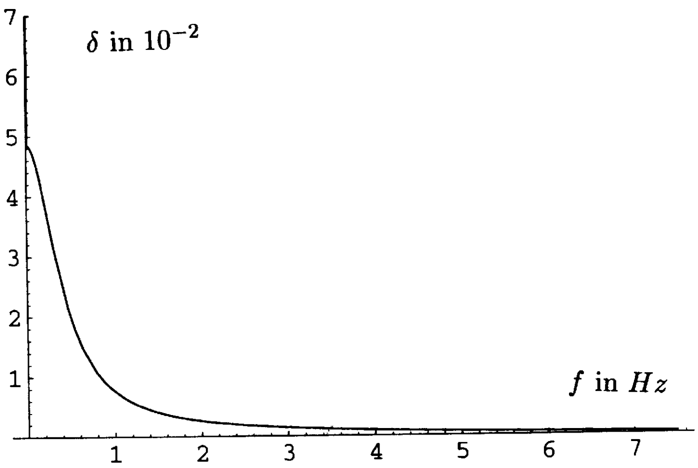

Figure 6. The ac-dc difference as a function of frequency for: $T_0 = 291$ K, $\alpha = 90 \times 10^{-6}$ K^{-1}, $\beta = 1{\cdot}5 \times 10^{-3}$ K^{-1}, $\rho_0 = 1{\cdot}08 \times 10^{-6}$ Ωm, $k_0 = 14$ W/(Km), $m = 8503$ kg/m^3, $s_0 = 435$ J/(kgK), $I = 0{\cdot}005$ A, $hl = 12{\cdot}6$, $a = 6{\cdot}36 \times 10^{-11}$ m^2, $\varepsilon = 0{\cdot}3$, $l = 2{\cdot}5 \times 10^{-3}$ m.

of the thermocouple). The experimental data tends to decrease with frequency faster that the theoretical curve.

In the Appendix B the result for δ is presented which is found by means of the eigenfunction-expansion method. Comparison of the two methods in Appendix C gives us some useful formulae for the summation of numerical series.

5. Conclusions

We have solved perturbatively the nonlinear heat-flow equation for the heater of the single-junction thermal converter. We have considered the two limiting cases: audio and low-frequency ranges. In the audio range, the treatment includes the previously neglected effects of radiation and the thermal properties of the heater wire. It is shown that the relative error caused by not taking the radiation into account is given by $RT_0^3(N+4)/3N$. If only the Thomson effect is taken into account we find an exact solution in terms of the Airy functions. In the low-frequency case, in addition to the nonlinearities of the heat flow equation, we include the thermal conductance of the thermocouple. Complete solutions are derived for both frequency ranges allowing accurate calculations of the ac-dc difference and clear design guidelines for SJTCs. Considering the problem at low frequencies by both the expansion in the eigenfunctions of the Sturm–Liouville problem and the Laplace transform, we have arrived at expressions for numerical series

$$\sum_{n=1}^{\infty} \frac{(-1)^n (2n-1)^{2k-1}}{(2n-1)^4 + a^4} \quad \text{and} \quad \sum_{n=1}^{\infty} \frac{(2n-1)^{2k}}{(2n-1)^4 + a^4}$$

that could be useful in other branches of science and engineering.

Table I. List of symbols

a	cross-sectional area of the heater wire	V_h	voltage across the heater
k	thermal conductivity of the heater	α	temperature coefficient of the heater resistivity
l	half-length of the heater wire	α_T	Thomson coefficient
m	density of the heater	β	temperature coefficient of thermal conductivity of the heater
p	perimeter of the heater wire		
s	specific heat of the heater	δ	ac-dc difference of the SJTC
t	time	ε	emissivity of the heater
I	heater current $I = I_{\rm dc}$ and $I = I_{\rm ac} = I_{\rm rms}\sin(\omega t)$ in the dc and ac cases, respectively	ζ	temperature coefficient of the specific heat of the heater
K	thermal conductance of the thermocouple	ρ	resistivity of the heater
R_{h0}	heater resistance at room temperature	σ	Stefan–Boltzmann constant
T	absolute temperature	ω	$2\pi f$ where f is the frequency of the ac source
T_0	room temperature		

Appendix A. Solution of heat equation with only Thomson term

If we neglect the radiation term and take $\alpha = \beta = \zeta = 0$ in (6), we can reduce (2) to the Ricatti equation

$$\frac{\mathrm{d}T(X)}{\mathrm{d}X} = p(X) = qT^2(X), \tag{A1}$$

where

$$X = x + C_1, \qquad p(X) = -\frac{I^2\rho}{a^2k}X, \qquad q = \frac{\beta_T I}{2ak}. \tag{A2}$$

Making the substitution $T = -w'/(qw)$, we get

$$w''(X) + p(X)qw(X) = 0. \tag{A3}$$

After solving (A2) we get for $-l \leqslant x \leqslant 0$ the following temperature distribution

$$T(x) = -\left(\frac{4\rho k}{\beta_T^2}\right)^{1/3} \frac{Ai'(z(x)) + C_2Bi'(z(x))}{Ai(z(x)) + C_2Bi(z(x))}, \qquad z(x) = \left(\frac{\beta_T}{(4\rho k)^2}\right)^{1/3} V_h\left(\frac{x}{l} + \frac{C_1}{l}\right), \tag{A4}$$

where $Ai(x)$, $Bi(x)$ are the Airy functions, C_1, C_2 are the integration constants, and $V_h = 2I\rho l/a$ is the volatage across the heater. By denoting the integration constants as C_3, C_4, the same expression (A3) is valid for the interval $0 \leqslant x \leqslant l$. Those constants are obtained by using the boundary conditions (3).

Appendix B. Result for δ at low frequencies by using the eigenfunction expansion

Using the eigenfunctions of the homogeneous part of (21) we can write it's solution as

$$\begin{aligned} u(x,t) &= -\frac{A_0 x^2}{2\tilde{k}} - \frac{A_0 l^2}{2\tilde{k}} \frac{hx}{1+hl} + \frac{A_0 l^2}{2\tilde{k}} \frac{1}{1+hl} \\ &+ \frac{4A_0 l^2}{\tilde{k}} \sum_{n=1}^{\infty} \frac{(1-\cos(\alpha_n l))\sin(\alpha_n (x+l))}{(\alpha_n l)^2 (\sin(2\alpha_n l) - 2\alpha_n l)} \\ &\times \left(\frac{\cos(2\omega t) + \frac{2\omega}{\tilde{k}\alpha_n^2} \sin(2\omega t)}{1 + \left(\frac{2\omega}{\tilde{k}\alpha_n^2}\right)^2} + \frac{\left(\frac{2\omega}{\tilde{k}\alpha_n^2}\right)^2}{1 + \left(\frac{2\omega}{\tilde{k}\alpha_n^2}\right)^2} \exp(-\tilde{k}\alpha_n^2 t) \right). \end{aligned} \tag{B1}$$

Following the similar steps as in the main part of the text we obtain for the ac-dc difference:

$$\delta = \sum_{n=1}^{\infty} Q_1(\alpha_n l) + \sum_{n=1}^{\infty} \sum_{m=n+1}^{\infty} Q_2(\alpha_n l, \alpha_m l),$$

$$\begin{aligned} Q_1(\alpha_n l) &= \eta \frac{A_0 l^2}{\tilde{k}} 2(1+hl) \frac{\sin(\alpha_n l)(1-\cos(\alpha_n l))}{\sin(2\alpha_n l) - 2\alpha_n l} \frac{1}{(\alpha_n l)^4 + \left(\frac{2\omega l^2}{\tilde{k}}\right)^2} \\ &+ \beta \frac{A_0 l^2}{\tilde{k}} 4 \left(\frac{1-\cos(\alpha_n l)}{\sin(2\alpha_n l) - 2\alpha_n l} \right)^2 \frac{(\alpha_n l)^2}{(\alpha_n l)^4 + \left(2\frac{\omega l^2}{\tilde{k}}\right)^2} \\ &\times \left(-\frac{1}{2} + \frac{1 - 2\alpha_n l \sin(2\alpha_n l) - \cos(2\alpha_n l)}{(2\alpha_n l)^2} \right) \\ &+ RT_0^2 \frac{A_0 l^2}{\tilde{k}} 24 \left(\frac{1-\cos(\alpha_n l)}{\sin(2\alpha_n l) - 2\alpha_n l} \right)^2 \frac{1}{(\alpha_n l)^4 + \left(2\frac{\omega l^2}{\tilde{k}}\right)^2} \\ &\times \left(-\frac{1}{2} - \frac{1 + 2\alpha_n l \sin(2\alpha_n l) + \cos(2\alpha_n l)}{(2\alpha_n l)^2} \right), \end{aligned} \tag{B2}$$

$$\begin{aligned} Q_2(\alpha_n l, \alpha_m l) &= \beta \frac{A_0 l^2}{\tilde{k}} 8 \frac{1-\cos(\alpha_n l)}{\sin(2\alpha_n l) - 2\alpha_n l} \frac{1-\cos(\alpha_m l)}{\sin(2\alpha_m l) - 2\alpha_m l} \\ &\times \frac{(\alpha_n l)(\alpha_m l) \left((\alpha_n l)^2 (\alpha_m)^2 + \left(2\frac{\omega l^2}{\tilde{k}}\right)^2 \right)}{\left((\alpha_n l)^4 + \left(2\frac{\omega l^2}{\tilde{k}}\right)^2 ((\alpha_m l)^4 + \left(2\frac{\omega l^2}{\tilde{k}}\right)^2 \right)} \end{aligned}$$

$$\times\left(\frac{1-(\alpha_n l-\alpha_m l)\sin(\alpha_n l-\alpha_m l)-\cos(\alpha_n l-\alpha_m l)}{(\alpha_n l-\alpha_m l)^2}\right.$$

$$\left.+\frac{1-(\alpha_n l+\alpha_m l)\sin(\alpha_n l+\alpha_m l)-\cos(\alpha_n l+\alpha_m l)}{(\alpha_n l+\alpha_m l)^2}\right)$$

$$+RT_0^2\frac{A_0 l^2}{\tilde{k}}48\frac{1-\cos(\alpha_n l)}{\sin(2\alpha_n l)-2\alpha_n l}\frac{1-\cos(\alpha_m l)}{\sin(2\alpha_m l)-2\alpha_m l}$$

$$\times\frac{(\alpha_n l)^2(\alpha_m l)^2+\left(2\frac{\omega l^2}{\tilde{k}}\right)^2}{\left((\alpha_n l)^4+\left(2\frac{\omega l^2}{\tilde{k}}\right)^2\right)\left((\alpha_m l)^4+\left(2\frac{\omega l^2}{\tilde{k}}\right)^2\right)}$$

$$\times\left(\frac{1-(\alpha_n l-\alpha_m l)\sin(\alpha_n l-\alpha_m l)-\cos(\alpha_n l-\alpha_m l)}{(\alpha_n l-\alpha_m l)^2}\right.$$

$$\left.-\left(\frac{1+(\alpha_n l+\alpha_m l)\sin(\alpha_n l+\alpha_m l)+\cos(\alpha_n l+\alpha_m l)}{(\alpha_n l+\alpha_m l)^2}\right)\right)$$

Equation (39) is a closed expression of (B2). Depending on precision required, up to 10 terms in (B2) produce the same result as (39).

Appendix C. Some useful numerical series formulae

By comparing the results obtained by the two approaches in the low frequency range, we get some simple enough expressions which probably frequently occur in science and engineering, and are candidates for inclusion in the standard tables of series[5] By comparing (B1) and (33) and taking the special case of $h = 0$, we have:

$$\frac{16}{\pi^3}\sum_{n=1}^{\infty}(-1)^n\frac{2n-1}{(2n-1)^4+\left(\frac{2\sqrt{2}\gamma l}{\pi}\right)^4}\cos\left((2n-1)\frac{\pi x}{2l}\right)$$

$$=\frac{(\sin(\gamma x)\sinh(\gamma x)\cos(\gamma l)\cosh(\gamma l)-\cos(\gamma x)\cosh(\gamma x)\sin(\gamma l)\sinh(\gamma l))}{(\gamma l)^2(\cosh(2\gamma l)+\cos(2\gamma l))},\qquad\text{(C1)}$$

$$\frac{128(\gamma l)^2}{\pi^5}\sum_{n=1}^{\infty}\frac{(-1)^n}{(2n-1)\left((2n-1)^4+\left(\frac{2\sqrt{2}\gamma l}{\pi}\right)^4\right)}\cos\left((2n-1)\frac{\pi x}{2l}\right)$$

$$=-\frac{1}{2(\gamma l)^2}\left[1-2\frac{\cos(\gamma x)\cosh(\gamma x)\cos(\gamma l)\cosh(\gamma l)+\sin(\gamma x)\sinh(\gamma x)\sin(\gamma l)\sinh(\gamma l)}{\cosh(2\gamma l)+\cos(2\gamma l)}\right],\qquad\text{(C2)}$$

[5] Some of the formulae below are actually generalizations of the corresponding entries in [13].

These relations can also be verified directly by expanding the right-hand sides into generalized Fourier serier by using the orthogonal bases $\cos((2n-1)\pi x/(2l))$ on the interval $-l \leqslant x \leqslant 0$. We obtain the first relation by twice differentiating the second relation with respeft to x. One can also see that this should be satisfied by substituting (34) in (18). By integrating and differentiating either of these equations and substituting the appropriate values for x, we obtain closed expressions for the numerical series of the form:

$$\sum_{n=1}^{\infty} \frac{(-1)^n (2n-1)^{2k-1}}{(2n-1)^4 + a^4}, \tag{C3}$$

and

$$\sum_{n=1}^{\infty} \frac{(2n-1)^{2k}}{(2n-1)^4 + a^4}, \tag{C4}$$

where $k = 0, \pm 1, \pm 2, \ldots$. Some examples are

$$\sum_{n=1}^{\infty} \frac{(2n-1)^2}{(2n-1)^4 + a^4} = \frac{\sqrt{2}\pi}{8a} \frac{\sinh\left(\frac{a\pi}{\sqrt{2}}\right) + \sin\left(\frac{a\pi}{\sqrt{2}}\right)}{\cosh\left(\frac{a\pi}{\sqrt{2}}\right) + \cos\left(\frac{a\pi}{\sqrt{2}}\right)},$$

$$\sum_{n=1}^{\infty} \frac{(-1)^{n+1}(2n-1)}{(2n-1)^4 + a^4} = \frac{\pi}{2a^2} \frac{\sinh\left(\frac{a\pi}{2\sqrt{2}}\right) \sin\left(\frac{a\pi}{2\sqrt{2}}\right)}{\cosh\left(\frac{a\pi}{\sqrt{2}}\right) + \cos\left(\frac{a\pi}{\sqrt{2}}\right)},$$

$$\sum_{n=1}^{\infty} \frac{1}{(2n-1)^4 + a^4} = \frac{\pi\sqrt{2}}{8a^3} \frac{\sinh\left(\frac{a\pi}{\sqrt{2}}\right) - \sin\left(\frac{a\pi}{\sqrt{2}}\right)}{\cosh\left(\frac{a\pi}{\sqrt{2}}\right) + \cos\left(\frac{a\pi}{\sqrt{2}}\right)},$$

$$\sum_{n=1}^{\infty} \frac{(-1)^{n+1}}{(2n-1)((2n-1)^4 + a^4} = \frac{\pi}{4a^4} \left(1 - 2\frac{\cosh\left(\frac{a\pi}{2\sqrt{2}}\right) \cos\left(\frac{a\pi}{2\sqrt{2}}\right)}{\cosh\left(\frac{a\pi}{\sqrt{2}}\right) + \cos\left(\frac{a\pi}{\sqrt{2}}\right)}\right),$$

$$\sum_{n=1}^{\infty} \frac{(-1)^{n+1}(2n-1)^3}{(2n-1)^4 + a^4} = \frac{\pi}{2} \frac{\cosh\left(\frac{a\pi}{2\sqrt{2}}\right) \cos\left(\frac{a\pi}{2\sqrt{2}}\right)}{\cosh\left(\frac{a\pi}{\sqrt{2}}\right) + \cos\left(\frac{a\pi}{\sqrt{2}}\right)},$$

$$\sum_{n=1}^{\infty} \frac{1}{(2n-1)^2((2n-1)^4 + a^4} = \frac{\pi^2}{8a^4} \left(1 - \frac{\sqrt{2}}{a\pi} \frac{\sinh\left(\frac{a\pi}{\sqrt{2}}\right) + \sin\left(\frac{a\pi}{\sqrt{2}}\right)}{\cosh\left(\frac{a\pi}{\sqrt{2}}\right) + \cos\left(\frac{a\pi}{\sqrt{2}}\right)}\right).$$

Acknowledgements

The author wishes to thank Dr. M. D. Early for valuable discussions.

References

1. F. C. Widdis, Theory of Peltier- and Thomson-effect errors in thermal AC-DC transfer devices. *Proc. Inst. Elec. Eng*. 109C (1956) 328–334.
2. B. D. Inglis, Standards for AC-DC transfer. *Metrologia* 29 (1992) 191–199.
3. F. L. Hermach, Thermal Converters as AC-DC Transfer standards for current and voltage measurements at audio frequences. *J. Res. Nat. Bur. Stand*. 48 (1952) 121–138.
4. B. D. Inglis and C. C. Franchimon, Current-independent AC-DC transfer errors in single junction thermal converters. *IEEE Trans. Instrum. Meas*. IM-34 (1985) 294–301.
5. H. S. Carslaw and J. C. Jaeger, *Conduction of Heat in Solids*. Oxford: Oxford University Press (1959) 510 pp.
6. P. B. Bailey, L. F. Shampine, and P. E. Waltman, *Nonlinear Two Point Boundary Value Problems*. New York: Academic Press (1968) 171 pp.
7. B. D. Inglis, A method for the determination of AC-DC transfer errors in thermoelements. *IEEE Trans. Instrum. Meas.* IM-27 (1978) 440–444.
8. H. Levinson, A computerised model of vacuum thermocouple performance. *IEEE Trans. Instrum.* 40 (1991) 356–359.
9. M. Klonz, T. Spiegel, R. Zirpel, B. D. Inglis, G. Hammond, H. Sasaki, K. Takahashi and B. Stojanović, Measuring thermoelastic effects in thermal converters with a fast reversed DC. *IEEE Trans. Instrum. Meas.* 44 (1995) 379–382.
10. H. Sasaki, B. D. Inglis, K. Takahaski, and M. Klonz, Determination of the time constants of thermoelectric effects in thermal converters using a fast-reverse DC. *IEEE Trans. Instrum. Meas.* 46 (1997) 377–381.
11. H. Sasaki, K. Takahashi, B. D. Inglis and M. Klonz, *A Numerical Simulation of Thermal Effects in Single-junction Thermal Converters*. Conference on Precision Electromagnetic Measurements CPEM98 Digest, Washington DC, July 1998, 169–170.
12. N. M. Oldham, S. Avramov-Zamurović, and M. E. Parker, Exploring the Low-Frequency Performance of Thermal Converters Using Circuit Models and a Digitally Synthesized Source. *IEEE Trans. Instrum. Meas*. IM-46 (1997) 352–355.
13. I. S. Gradshteyn and I. M. Ryzhik, *Table of Integrals Series, and Products*. New York: Academic Press (1994) 1204 pp.